Aus dem

Institut für Prophylaxe und Epidemiologie der Kreislaufkrankheiten (IPEK)

Klinik der Ludwig-Maximilians-Universität München

Direktor: Prof. Dr. Christian Weber

Macroscopic in vivo imaging in the shortwave infrared: technological innovations and biological applications

Dissertation
zum Erwerb des Doktorgrades der Naturwissenschaften
an der Medizinischen Fakultät der
Ludwig-Maximilians-Universität München

vorgelegt von
Bernardo Caetano Assein Arús

aus
Rio Grande (Brasilien)

Jahr
2025

Mit Genehmigung der Medizinischen Fakultät
der Ludwig-Maximilians-Universität München

Betreuer:	Prof. Dr. Alexander Bartelt
Zweitgutachter:	Prof. Dr. Markus Rehberg
Dekan:	Prof. Dr. med. Thomas Gudermann
Tag der mündlichen Prüfung:	03. Februar 2026

LMU LUDWIG-MAXIMILIANS-UNIVERSITÄT MÜNCHEN

Dekanat Medizinische Fakultät
Promotionsbüro

Affidavit

Caetano Assein Arús, Bernardo

Surname, first name

I hereby declare, that the submitted thesis entitled

Macroscopic in vivo imaging in the shortwave infrared:
technological innovations and biological applications

is my own work. I have only used the sources indicated and have not made unauthorised use of services of a third party. Where the work of others has been quoted or reproduced, the source is always given.

I further declare that the dissertation presented here has not been submitted in the same or similar form to any other institution for the purpose of obtaining an academic degree.

Munich, 09.02.2026

Place, Date

Bernardo Caetano Assein Arús

Signature doctoral candidate

LMU LUDWIG-MAXIMILIANS-UNIVERSITÄT MÜNCHEN

Dekanat Medizinische Fakultät
Promotionsbüro

Confirmation of congruency between printed and electronic version of the doctoral thesis

Doctoral candidate: Bernardo Caetano Assein Arús

Address:

I hereby declare that the electronic version of the submitted thesis, entitled

Macroscopic in vivo imaging in the shortwave infrared: technological innovations and biological applications

is congruent with the printed version both in content and format.

Munich, 09.02.2026 — Bernardo Caetano Assein Arús

Place, Date — Signature doctoral candidate

Table of contents

List of abbreviations

Abbreviation	Definition
ICG	indocyanine green
InGaAs	indium gallium arsenide
iRFP	near-infrared fluorescent proteins
NADH	Nicotinamide adenine dinucleotide
NIR	near infrared
Si	silicon
SWIR	shortwave infrared

List of publications

Peer-reviewed publications featured in this thesis

Article 1: Cosco ED, Spearman AL, Ramakrishnan S, Lingg JGP, Saccomano M, Pengshung M, Arús BA, Wong KCY, Glasl S, Ntziachristos V, Warmer M, McLaughlin RR, Bruns OT, Sletten EM. Shortwave infrared polymethine fluorophores matched to excitation lasers enable non-invasive, multicolour *in vivo* imaging in real time. *Nature Chemistry.* 2020, 12(12), 1123-1130.

Article 2: Cosco ED, Arús BA, Spearman AL, Atallah TL, Lim I, Leland OS, Caram JR, Bischof TS, Bruns OT, Sletten EM. Bright chromenylium polymethine dyes enable fast, four-color *in vivo* imaging with shortwave infrared detection. *Journal of the American Chemical Society*. 2021, 143(18), 6836-6846.

Article 3: Arús BA, Cosco ED, Yiu J, Balba I, Bischof TS, Sletten EM, Bruns OT. Shortwave infrared fluorescence imaging of peripheral organs in awake and freely moving mice. *Frontiers in Neuroscience.* 2023, 17, 1135494.

Article 4: Arteaga Cardona F, Jain N, Popescu R, Busko D, Madirov E, Arús BA, Gerthsen D, De Backer A, Bals S, Bruns OT, Chmyrov A, Van Aert S, Richards BS, Hudry D. Preventing cation intermixing enables 50% quantum yield in sub-15 nm short-wave infrared-emitting rare-earth based core-shell nanocrystals. *Nature Communications.* 2023, 14(1), 4462.

Article 5: Arteaga Cardona F, Madirov E, Popescu R, Wang D, Busko D, Ectors D, Kübel C, Eggeler YM, Arús BA, Chmyrov A, Bruns OT, Richards BS, Hudry D. Dramatic impact of materials combinations on the chemical organization of core–shell nanocrystals: boosting the Tm^{3+} emission above 1600 nm. *ACS Nano*. 2024, 18(38), 26233–26250.

Pre-print research articles featured in this thesis

Article 6 (Appendix): Xu C*, Liu Y*, Arús BA*, Mishra K*, Luciano M, Bandi V, Kumar A, Guo Z, Bick M, Xu M, Zhang K, Lingg J, Bae J, Kang A, Gerben SR, Bera AK, Vaughan JC, Manton JD, Derivery E, Schnermann MJ, Stiel AC, Bruns OT, Baker D. De novo design of near infrared fluorescent proteins. *Research Square*. 2024, 4652998.

* shared first authorship

Article 7 (Appendix): Arús BA, Yiu J, Lingg JGP, Hofmann A, Fumo AR, Ji H, Jethwa C, Park R K, Henderson J, Mishra K, Mukha I, Stiel AC, Santovito D, Weber C, Reeps C, Rohm M, Bartelt A, Valdez TA, Chmyrov A, Bruns OT. Macroscopic label-free biomedical imaging with shortwave infrared Raman scattering. *bioRxiv*. 2024, 10597863.

Additional peer-reviewed publications

Lingg, JGP, Bischof, T S, Arús, BA, Cosco, ED, Sletten, EM, Rowlands, CJ, Bruns, OT, Chmyrov, A. Shortwave-infrared line-scan confocal microscope for deep tissue imaging in intact organs. *Laser Photonics Reviews.* 2023, 17(11), 2300292.

Luo J, Molbay M, Chen Y, Horvath I, Kadletz K, Kick B, Zhao S, AlMaskari R, Singh I, Ali M, Bhatia HS, Minde DP, Negwer M, Hoeher L, Calandra GM, Groschup B, Su J, Kimna C, Rong Z, Galensowske N, Todorov MI, Jeridi D, Ohn TL, Roth S, Simats A, Singh V, Khalin I, Pan C, Arús BA, Bruns OT, Zeidler R, Liesz A, Protzer U, Plesnila N, Ussar S, Hellal F, Paetzold J, Elsner M, Dietz H, Erturk A. Nanocarrier imaging at single-cell resolution across entire mouse bodies with deep learning. *Nature Biotechnology.* 2025, 43, 2009-2022.

Additional pre-print research articles

Jethwa C, Hoffmann A, Kotschi S, Caesar J, Kern M, Worthmann A, Schlein C, Khani S, Arús BA, Bruns OT, Ghosh A, Wolfrum C, Döring Y, Herzig S, Weber C, Blüher M, Widenmaier SB, Hotamışlıgil GS, Bartelt A. Control of cholesterol-induced adipocyte inflammation by the Nfe2l1-Atf3 pathway. *bioRxiv.* 2024, 22604614.

1 My contribution to the publications

1.1 Contribution to Article 1

For the article with the title “Shortwave infrared polymethine fluorophores matched to excitation lasers enable non-invasive, multicolour *in vivo* imaging in real time” published in Nature Chemistry in 2020, in collaboration with EDC, I performed dye encapsulation in micelles, *in vivo* and *ex vivo* imaging experiments, as well as data processing and analysis. In particular, I was instrumental for the study of the resolution effects between excitation and emission multiplexing in the shortwave infrared spectral region.

1.2 Contribution to Article 2

For the article with the title “Bright chromenylium polymethine dyes enable fast, four-color *in vivo* imaging with shortwave infrared detection” published in the Journal of the American Chemical Society in 2021, in collaboration with EDC, I co-led the design and implementation of the imaging experiments that characterized the fluorophores’ biodistribution and evaluated their *in vivo* performance for fast and multiplexed imaging. With input from OTB, I optimized the imaging system to improve multiplexing performance during raw data acquisition, eliminating the need for post-processing steps like linear unmixing to distinguish multiple fluorophores *in vivo*. Moreover, I acquired all of the imaging data, and played a major role in imaging data processing and analysis. I co-wrote the imaging methods section and provided input in the manuscript draft provided by EDC.

1.3 Contribution to Article 3

For the article with the title “Shortwave infrared fluorescence imaging of peripheral organs in awake and freely moving mice”, published in Frontiers in Neuroscience in 2023, I led the study conceptualization and design with input from OTB and EDC, further optimized the data acquisition and processing workflows, performed all *in vivo* imaging experiments, and processed and analyzed the data. Moreover, I wrote the full draft of the manuscript, worked on further edits after input from the co-authors, and prepared all figures and videos. For publication, I revised the manuscript with input from OTB, and co-led the correspondence with editor and reviewer.

1.4 Contribution to Article 4

For the article with the title “Preventing cation intermixing enables 50% quantum yield in sub-15 nm short-wave infrared-emitting rare-earth based core-shell nanocrystals”, published in Nature Communications in 2023, I conceptualized and led the *in vivo* imaging experiments with input from OTB and AC. I assembled an imaging system with high-sensitivity to detect the nanocrystals’ emission at wavelengths beyond 1450 nm and provide whole-body mouse angiography. Besides acquiring, processing and analyzing the *in vivo* imaging data, I also contributed to the establishment of a phase-transfer protocol for biocompatibility. Moreover, I prepared the figure and wrote the imaging methods section.

1.5 Contribution to Article 5

For the article with the title “Dramatic impact of materials combinations on the chemical organization of core–shell nanocrystals: boosting the Tm^{3+} emission above 1600 nm”, published in ACS Nano in 2024, I designed, implemented and optimized the imaging system based on an extended InGaAs detector for the macroscopic detection of thulium emission between 1600 and 2000 nm, which will enable *in vivo* experiments in future studies. In addition, I conceptualized and executed the depth and contrast experiments that compared the *in vitro* performance of erbium- and thulium-based nanocrystals in tissue phantoms. For publication, I prepared the figure for this experiment and wrote the imaging methods section.

1.6 Contribution to Article 6 (Appendix)

For the article with the title “De novo design of near infrared fluorescent proteins”, I conceptualized and led the imaging experiments with input from OTB. I set up a back-illuminated silicon-based macroscopic imaging system able to detect wavelengths ranging from the visible to 1100 nm for the visualization of fluorescent proteins with emission in the green, near-infrared, and shortwave infrared regions. Moreover, I characterized the emission of the isolated fluorescent proteins as well as in the alginate beads through both imaging and spectroscopic measurements, and performed the animal procedures and *in vivo* imaging experiments. Finally, I analyzed the data, prepared the macroscopic imaging figures, and drafted the methods and results sections relative to macroscopic fluorescence imaging.

1.7 Contribution to Article 7 (Appendix)

For the article with the title “Macroscopic label-free biomedical imaging with shortwave infrared Raman scattering”, I conceptualized and led the project with input from OTB and AC. I co-designed with AC the high-sensitivity SWIR imaging approach that eventually enabled high-contrast macroscopic imaging of spontaneous Raman scattering. I performed the animal work, and spearheaded with OTB the collaborations to source biological samples and models to validate the system. In addition, all imaging and spectroscopic experiments were performed by me and/or by JY under my supervision. I also conducted all data processing and analysis. Finally, I wrote the full draft of the manuscript, worked on further edits after input from the co-authors, and prepared all figures.

2 Introduction

Biomedical imaging integrates principles from physics, chemistry, engineering, biology, and medicine to improve disease detection and diagnosis, surgical guidance, and treatment monitoring (Webb 2022). Accordingly, biomedical imaging techniques are widely used in clinical and pre-clinical research, supporting scientists and clinicians in investigating disease mechanisms, evaluating new treatments and diagnostic approaches, and refining surgical procedures (Weissleder and Nahrendorf 2015, Cheng, Xu et al. 2024). Common imaging methods include magnetic resonance imaging, x-ray, computed tomography, positron emission tomography, and various optical imaging approaches (James and Gambhir 2012, Wallyn, Anton et al. 2019, Webb 2022).

The research articles featured in this thesis advance the instrumentation and applications of two optical modalities: fluorescence and Raman scattering imaging. By exploring these techniques in the shortwave infrared (SWIR) spectral region (1000 to 2000 nm), novel macroscopic biomedical imaging applications have been enabled, constituting the central theme connection the articles (Figure 1). This chapter introduces key concepts covered in these articles, including SWIR-emissive fluorophores (Articles 1-5), fluorescent proteins (Article 6), and Raman scattering imaging (Article 7), and concludes by outline the primary objectives of the thesis.

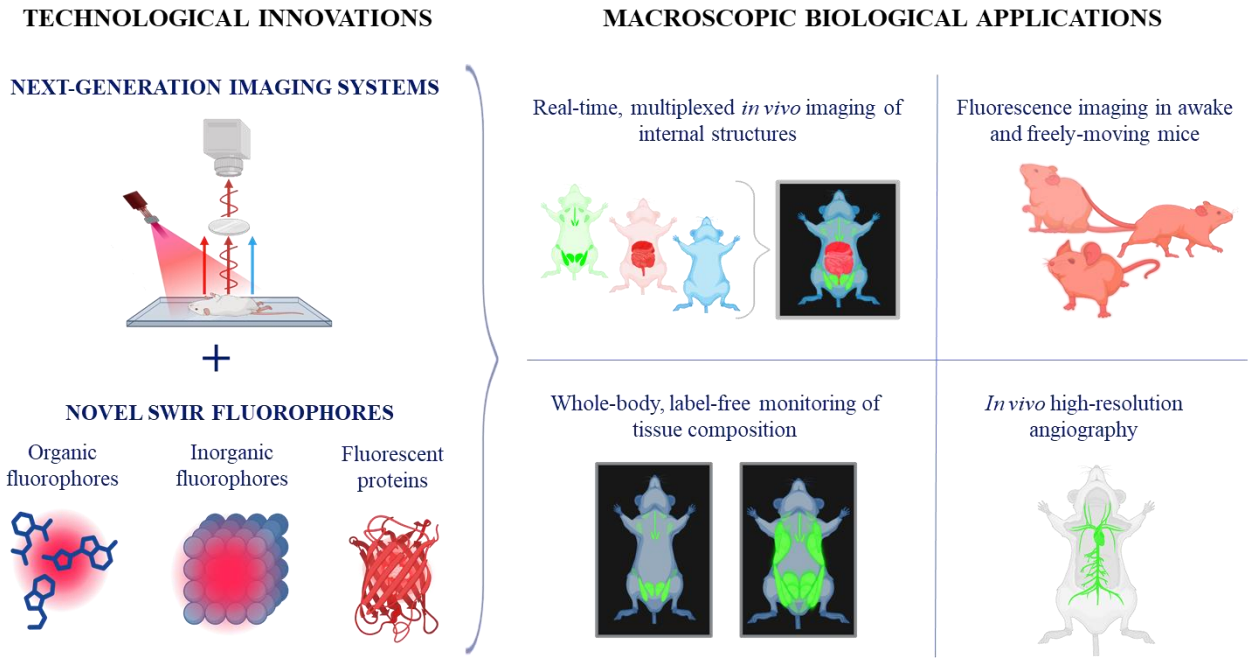

Figure 1. Graphical abstract. The development of next-generation macroscopic shortwave infrared (SWIR) imaging systems and novel enables advanced biological applications.

2.1 Fluorescence imaging in the shortwave infrared

Fluorescence imaging is a powerful tool in biomedical research and clinical practice for visualizing and tracking specific molecules and structures within biological tissues, providing insights into

molecular and cellular dynamics during disease progression and offering anatomical guidance during surgeries (Resch-Genger, Grabolle et al. 2008, Mieog, Achterberg et al. 2022, Refaat, Yap et al. 2022). This technique relies on the property of certain molecules, called fluorophores, to emit light upon photon absorption at specific wavelengths, allowing for real-time monitoring of biological processes (Lakowicz 2006).

Traditionally, fluorescence imaging has been performed in the near-ultraviolet (200 to 380 nm), visible (380 to 700 nm) and near-infrared (NIR, 700 to 1000 nm) spectral regions (Refaat, Yap et al. 2022). These ranges are compatible with many commercially available fluorophores and detection systems, often based on silicon (Si) (Zhu, Kwon et al. 2020). However, there has been a significant growth in biomedical imaging using the SWIR spectral window over the past decades, thus requiring detectors that are sensitive beyond the detection range of Si, such as those based on indium gallium arsenide (InGaAs) (Chen, Wang et al. 2023). This increase in interest in SWIR biological imaging is primarily driven by its unique photophysical advantages, when compared to imaging at shorter wavelengths (Schmidt, Ou et al. 2024, Wang, Zhong et al. 2024). For instance, SWIR benefits from lower tissue scattering, increased water absorption, and lower tissue autofluorescence, ultimately providing deeper tissue penetration and enhanced image contrast (Wilson, Nadeau et al. 2015, Carr, Aellen et al. 2018) (Figure 2).

Image contrast in fluorescence is crucial to distinguish labeled structures from the tissue background. Tissue autofluorescence, which arises from the natural emission of light by endogenous biomolecules when they are excited by light, is a key type of background that exogenous fluorophores need to overcome (del Rosal and Benayas 2018). In visible and NIR imaging, autofluoresence configures the main source of biological background (del Rosal, Thomas et al. 2020). Common endogenous fluorophores include nicotinamide adenine dinucleotide (NADH), porphyrins, melanin, and lipofuscin (Croce and Bottiroli 2014). Although the precise sources and behavior of autofluorescence in the SWIR range are not well understood, particularly above 800 nm excitation, it is accepted that fewer endogenous fluorophores are excited at these wavelengths, leading to a decreased autofluorescence emission as the wavelength increases (Del Rosal, Villa et al. 2016, del Rosal, Thomas et al. 2020, Sun, Zhong et al. 2023). In this thesis, Article 6 highlights the advantage of longer wavelength excitation by showing that fluorescent beads injected into the mouse peritoneum are visualized when excited at 892 nm but are completely obscured by autofluorescence when excited at 672 nm. Moreover, Article 7 demonstrates that SWIR autofluorescence is so low that Raman scattering, a very weak spontaneous effect of light-tissue interaction, becomes the dominant source of tissue background at longer wavelengths. Lower autofluorescence results in the ability to detect lower doses of exogenous fluorophores in tissue, therefore reducing potential risks associated with contrast agent administration.

Overcoming autofluorescence is relatively simple and can be achieved by selecting brighter fluorophores or increasing their concentration. However, a more significant challenge is the contrast limitation posed by the signal-to-background ratio, which defines the relationship between the fluorescence signals from the target structure against those of the surrounding tissue, (Judy, Keating et al. 2015). Moreover, a major effect of light-tissue interactions that impairs contrast is scattering, which occurs when light changes direction upon interacting with microscopic structures

such as cells, fibers, or macromolecules (Wilson, Nadeau et al. 2015). The effects of scattering reduce image clarity by causing blurriness, and limits penetration depth, making it difficult to resolve fine details or visualize structures deeper within tissues (Frangioni 2003).

The inverse relationship between scattering and wavelength makes switching to SWIR wavelengths a promising strategy to overcome contrast and penetration depth limitations common in visible and NIR fluorescence imaging (Frangioni 2003, Wang, Zhong et al. 2024). In addition, SWIR wavelengths benefit from strong water absorption, which can further improve contrast by absorbing scattered photons (Carr, Aellen et al. 2018). This combination of reduced scattering and strong water absorption makes SWIR imaging particularly valuable for applications requiring high resolution of fine structures in deeper tissue layers, such as angiography and nerve imaging (Hong, Diao et al. 2014, Carr, Aellen et al. 2018). Although imaging at highly absorbing wavelengths has traditionally been avoided due to concerns about low photon detection, these challenges can often be addressed by increasing fluorophore concentrations or boosting illumination power. Nevertheless, these adjustments do not enhance the signal-to-background ratio, as both the target and background signals will increase proportionally. Therefore, improving contrast is critical to advancing fluorescence imaging, and the unique photophysical properties of SWIR offer a powerful solution to this challenge.

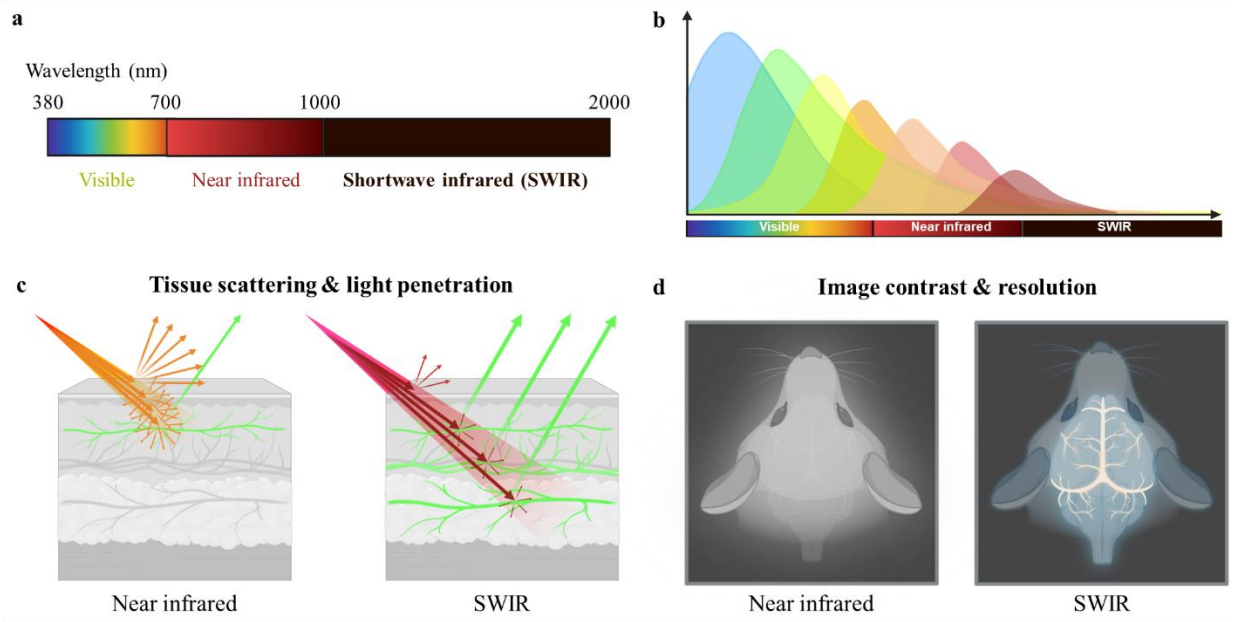

Figure 2. Photophysical advantages of shortwave infrared (SWIR) imaging compared to visible and near-infrared (NIR) imaging. **a)** Section of the electromagnetic spectrum, highlighting the visible, NIR and SWIR regions. **b)** Schematic representation of autofluorescence emission profiles of endogenous tissue chromophores across the spectral regions. As wavelength increases, excitation of chromophores decreases, resulting in lower autofluorescence in the SWIR. **c)** Comparison of light-tissue interactions between NIR and SWIR illumination, respectively represented in orange and dark red. SWIR light scatters less due to the inverse relationship between scattering and wavelength, allowing for the excitation of fluorescently-labeled structures (green) deeper in the tissue. **d)** Schematic illustration of the increased contrast in SWIR fluorescence images. Reduced photon scattering, combined with water absorption of scattered photons, improves image clarity and resolution of fine structures.

The contrast advantages of SWIR imaging have been thoroughly demonstrated in both animals and humans studies, particularly in research comparing the SWIR emission tail of NIR contrast agents with their NIR peaks (Carr, Franke et al. 2018, Hu, Fang et al. 2020, Wu, Suo et al. 2022). Despite capturing only a small portion of the fluorophore's emission in the SWIR range, this spectral region has consistently revealed more blood vessels with greater resolution than the NIR wavelengths commonly used in clinical imaging. This thesis highlights the high-contrast and deep penetration capabilities of SWIR fluorescence imaging *in vitro* (Article 5), along with a wide range of enabled biological applications, including multiplexed deep-tissue imaging in both anesthetized (Articles 1-2) and awake, freely moving mice (Article 3), as well as high-resolution whole-body vascular imaging at emission wavelengths beyond 1450 nm (Article 4).

2.2 Shortwave infrared-emitting fluorophores and imaging systems

While most commercial fluorophores are optimized for the ultraviolet and visible regions, efforts to expand fluorescent imaging to longer wavelengths have driven the development of red-shifted fluorophores with NIR excitation at around 800 nm, especially for *in vivo* applications (Grimm and Lavis 2022). Clinically approved NIR fluorophores, such as indocyanine green (ICG) and IRDye 800 CW, are well established in surgical applications, with ongoing clinical trials exploring new molecules to enhance fluorescence imaging capabilities (Alander, Kaartinen et al. 2012, Zhang, Schroeder et al. 2017). Notably, many NIR fluorophores, including ICG, exhibit an emission tail in the SWIR range (Carr, Franke et al. 2018). To further improve imaging performance in this spectral window, recent research has increasingly focused on developing fluorophores with excitation wavelengths beyond 800 nm and emission peaks closer to or beyond 1000 nm (Welsher, Liu et al. 2009, Piwonski, Nozue et al. 2022, Wang, Zhong et al. 2024).

Multiplexed imaging is a key goal in advancing SWIR fluorophores and imaging systems, being highly valuable in both surgical and *in vivo* research settings (Okamoto, Al-Difaie et al. 2023, Heuvelings, Scheepers et al. 2024, Zhong, Patel et al. 2024). In surgery, it could enable the simultaneous labeling and contrast enhancement of multiple structures, including nerves, tumors, as well as blood and lymph vessels. In research, multiplexing could offer the ability to non-invasively visualize and monitor tissue dynamics, such as macrophage polarization, collagen deposition, and vascularization, providing real-time feedback on tissue composition during disease progression and/or treatment efficacy. Multiplexing requires the use of spectrally distinct fluorophores and different imaging channels, which may involve various combinations of illumination source, detectors, or emission filters (Bandi, Luciano et al. 2022).

Furthermore, fast acquisition times are essential to avoid motion artifacts, particularly in real-time surgical applications or when imaging tissue dynamics in freely moving animals. Achieving high signal-to-noise ratios at short exposure times requires bright fluorophores, especially for wavelengths above 1400 nm, where tissue water absorption is strong, but optimal contrast can be achieved (Carr, Aellen et al. 2018). However, SWIR fluorophores generally exhibit lower brightness than their visible and NIR counterparts due to their reduced energy gap, which reduces quantum yields (Ding, Zhan et al. 2018, Zhu, Tian et al. 2019, Wang, Zhong et al. 2024).

SWIR fluorophores can be broadly categorized into organic and inorganic dyes. Organic fluorophores, such as small molecules like polymethine dyes and donor-acceptor systems, generally offer better biocompatibility than inorganic dyes, making them more suitable for *in vivo* applications and clinical translation (Piwonski, Nozue et al. 2022, Ou, Ren et al. 2023, Martin and Rivera-Fuentes 2024). However, organic dyes mostly emit below 1200 nm and often exhibit lower quantum yields, which poses a limitation for fast SWIR imaging (Ou, Ren et al. 2023). In contrast, inorganic dyes, such as quantum dots and rare-earth nanocrystals, can reach emission peaks beyond 1400 nm for improved imaging contrast, but increasing their brightness remains essential for fast imaging in high-absorbing wavelengths (Liu, Li et al. 2022). Therefore, ongoing research focuses on expanding the emission range and improving quantum yields, photostability, and specificity of both organic and inorganic SWIR contrast agents to achieve high brightness and open up new channels for multiplexed imaging (Liu, Li et al. 2022, Schmidt, Ou et al. 2024). This thesis introduces major advancements in the development of both organic and inorganic SWIR contrast agents, along with novel biological applications. Customized imaging systems are designed for each application, leading to progress in both fluorophore development and SWIR imaging instrumentation.

Among organic fluorophores, polymethine dyes are particularly valuable for *in vivo* multiplexed SWIR imaging, due to their narrow absorption bands, high absorption coefficients, and increased photostability (Blua, Boccalon et al. 2024, Martin and Rivera-Fuentes 2024).. Recently, flavylium-based polymethine dyes have emerged as a powerful class of organic fluorophores with tunable properties for high-contrast, deep tissue imaging in the SWIR range (Cosco, Caram et al. 2017, Uranga-Barandiaran, Casanova et al. 2020, Blua, Boccalon et al. 2024). In this thesis, Articles 1 and 2 introduce a library of novel penta- and heptamethine dyes with flavylium and chromenylium heterocycles featuring excitation ranges from 785 to 1064 nm, offering enhanced brightness that enabled unprecedented *in vivo* imaging speeds of up to 300 frames per second. These articles also present an innovative excitation multiplexing strategy, which optimizes illumination wavelengths tailored for each fluorophores' absorbance, while maintaining with a single detection window. This approach effectively prevents the strong chromatic aberrations associated with SWIR wavelengths (Article 1), and removes the need for filter changes, which speeds up acquisition. Furthermore, the strategic balance between laser power and dye concentrations significantly minimizes emission crosstalk among the fluorophores, thereby precluding the need for post-processing steps such as spectral unmixing (Article 2). These articles demonstrate that the combination of increased fluorophore brightness and tailored imaging enables the simultaneous labeling and real-time visualization of structures such as lymph vessels, blood vasculature, intestines, and bones in up to four channels. Notably, this approach further enables imaging of multiple structures in freely moving mice, maintaining resolution even in fast-motion conditions (Article 3), thus opening up possibilities to study physiological processes without the confounding effects of anesthesia. Together, Articles 1-3 expand the multiplexing capabilities and applications of *in vivo* SWIR imaging, allowing for real-time visualization of multiple structures with minimal crosstalk at unprecedented speeds and number of imaging channels.

In parallel with the development of organic fluorophore, this thesis presents significant progress in inorganic SWIR dyes, specifically erbium- and thulium-doped rare-earth nanocrystals, for high-contrast imaging applications beyond 1450 nm. Article 4 highlights improvements in the photophysical performance of erbium-based nanocrystals, which emit around 1550 nm when excited near 980 nm. This article shows that implementing a heterogeneous shell domain to optically-active erbium-based core nanocrystals provides a substantial boost in quantum yield, achieving 50% for sub-15 nm nanocrystals under safe illumination levels, a remarkable achievement. Using micelle formulations for solubility in water, these nanocrystals are administered intravenously and imaged with a sensitive, liquid nitrogen-cooled InGaAs detector. Displaying its biocompatibility, brightness and image clarity, this strategy enables *in vivo* multi-color angiography at the whole-body scale, providing a comprehensive visualization of vascular structures with high resolution.

Imaging at 1550 nm particularly benefited from high water absorptivity, which improved image contrast by absorbing background fluorescence and scattered light. With the goal to develop materials with emission in a spectral regions with even lower influence of tissue scattering and higher water absorptivity, Article 5 presents pioneering work on thulium-doped nanocrystals for fluorescence imaging between 1600 and 2000 nm upon excitation near 785 nm, which require a specialized imaging system using an extended InGaAs detector. By optimizing the core-shell material combination, a quantum yield of 39% is achieved, an unprecedented feature for emission at these wavelengths. SWIR imaging of these materials in tissue phantoms shows that deeper penetration up to 1 cm and higher contrast is achieved for the thulium-based nanocrystals, when compared to the erbium-based ones. While *in vivo* imaging has not been performed, this work paves the way for novel fluorophores and applications in an underexplored spectral window for biological imaging.

Furthermore, fluorescent proteins are another class of fluorophores extensively used in biological research for visualizing cellular and molecular processes, from high-resolution microscopy to whole-body imaging (Hoffman 2005, Rodriguez, Campbell et al. 2017). A major advantage of fluorescent proteins over traditional exogenous fluorophores is their ability to be genetically encoded, which allows for precise labeling and visualization of specific cellular structures, due to the possibility to target the protein expression in defined cells and tissues (Rodriguez, Campbell et al. 2017). Moreover, endogenous expression circumvents the need for external administration, highlighting the non-invasive nature of fluorescent protein imaging in living organisms. Since the discovery of fluorescent proteins, intense engineering efforts have been applied to create a library of proteins with emission across the whole visible spectrum (Chudakov, Matz et al. 2010). More recently, near-infrared fluorescent proteins (iRFPs), emitting in the far red and NIR between 670 and 720 nm, were developed to capitalize on the benefits of imaging at longer wavelengths (Chudakov, Matz et al. 2010, Filonov, Piatkevich et al. 2011).

Notably, like ICG, iRFPs exhibit an emission tail in the SWIR region, offering increased contrast at these wavelengths (Chen, Feng et al. 2022, Oliinyk, Ma et al. 2023). Despite this advancement, a considerable gap remains in fluorescent proteins optimized specifically for SWIR emission, limiting their utility in deeper tissue imaging applications compared to SWIR organic

and inorganic fluorophores. Addressing this gap, Article 6 in this thesis introduces a pioneering SWIR-emitting fluorescent protein, MC9BP81, with excitation at 892 nm. This novel protein, designed to bind a synthetic merocyanine dye, demonstrates higher contrast and *in vivo* imaging sensitivity compared to iRFP720, which excites at around 700 nm. In a comparative study, alginate beads containing cells expressing both MC9BP81 and iRFP720 are injected into the mouse peritoneum. Although iRFP exhibits higher brightness, the beads remain undetectable due to the dominant autofluorescence from the abdominal region at 672 nm excitation. In contrast, MC9BP81 fluorescence enable the clear resolution of the beads, benefitting from the reduced autofluorescence at 892 nm excitation. Altogether, the introduction of an engineered SWIR fluorescent protein sets a foundation for a new class of genetically encoded probes, expanding possibilities for non-invasive, deep-tissue imaging and enabling more refined visualization of biological processes in pre-clinical research.

2.3 Macroscopic SWIR Raman imaging

Raman scattering is a weak spontaneous physical effect that arises from the exchange of energy between incoming photons and chemical bonds within molecules (Cialla-May, Schmitt et al. 2019). This energy exchange results in distinctive spectral shifts for each type of chemical bond, expressed as wavenumber in inverse centimeters (cm^{-1}). Detecting such spectral shifts can be utilized to extract the chemical composition and structure of materials of interest, including biological tissues, allowing for the label-free visualization of individual biomolecules within tissues and cells solely based on endogenous tissue chemical contrast (Hu, Shi et al. 2019). Particularly using strategies for enhancing the Raman scattering intensity, Raman imaging techniques have offered powerful label-free capabilities in both clinical and pre-clinical settings (Freudiger, Min et al. 2008, Palonpon, Ando et al. 2013, Kong, Kendall et al. 2015, Orringer, Pandian et al. 2017).

However, as these approaches require high laser fluxes onto small sample areas, their application has been confined to the microscopic scale (Krafft, Schie et al. 2016). For example, microscopy based on coherent Raman imaging requires high laser fluxes, practically limiting them to the laser focal point, which is on the order of millimeters (Krafft, Schie et al. 2016, Hu, Shi et al. 2019). Moreover, spectroscopic detection of spontaneous Raman scattering involves illumination at a single point or along a line, and it requires minutes in order to scan a field of only 1 cm^2 (Bohndiek, Wagadarikar et al. 2013). Expanding Raman imaging to large fields of view would allow for the comprehensive analysis of heterogeneous tissues, with significant potential applications in whole-body animal studies and medical procedures such as surgical contexts (Jermyn, Mok et al. 2015, Wilson, Jermyn et al. 2018).

Wide-field Raman imaging shows promise for expanding the field of view, but typical silicon-based detection systems are hindered by tissue autofluorescence (Yang, Li et al. 2014, Papour, Kwak et al. 2015). As illumination wavelength increases, autofluorescence decreases (Patil, Pence et al. 2014, Sun, Zhong et al. 2023). Researchers have implemented wide-field Raman systems with NIR illumination wavelengths, typically 785 nm, to reduce autofluorescence while maintaining detectable Raman scattering shifts within Si-based detection limits (Papour, Kwak et

al. 2015, Krafft, Schie et al. 2016, Wei, Chen et al. 2016), but achieving satisfactory chemical contrast for wide-field imaging remains an unmet need.

In this thesis, Article 7 introduces the discovery that Raman scattering can surpass autofluorescence as the predominant source of tissue background at illumination wavelengths starting from 892 nm, with chemical contrast further increasing as the illumination reaches up to 1064 nm. These longer wavelengths shift the Raman scattering of various biomolecules into the SWIR range, thus requiring SWIR-sensitive detectors. Article 7 describes the design and implementation of a highly sensitive, wide-field SWIR system capable of acquiring Raman images at an unprecedented spatial scale and with remarkable chemical contrast in just a few seconds of exposure. This imaging system enables a range of label-free, macroscopic applications across both preclinical and clinical settings. Notably, SWIR Raman imaging allows for the longitudinal, *in vivo* tracking of dynamic changes in body composition at the whole-mouse scale, such as adipose tissue mobilization during fasting and refeeding, as well as the non-invasive detection of fatty liver disease. Additionally, SWIR Raman imaging enables the visualization of calcified and lipid-rich regions within fresh, unfixed human atherosclerotic plaques, offering valuable, complementary insights to traditional histology by capturing tissue heterogeneity prior to tissue processing. With its large field of view and high chemical specificity, SWIR Raman imaging also holds promise in surgical applications, as demonstrated by its capacity to identify nerves embedded within fatty tissue in a porcine model. In summary, Article 7 addresses a critical limitation of traditional Raman imaging by enabling high chemical contrast over larger areas in a straightforward wide-field configuration that detects Raman scattering in the SWIR range, establishing SWIR Raman imaging as a versatile tool in both pre-clinical and clinical research.

2.4 Research aims

The overarching goal of this thesis is to advance SWIR technology development for innovative macroscopic applications in the life sciences. This goal is achieved by setting seven specific aims:

- Aim I: develop and investigate novel SWIR-emitting polymethine dyes for enhanced *in vivo* multiplexed imaging capabilities (Articles 1 and 2)
- Aim II: implement imaging strategies to achieve fast, real-time, multiplexed imaging in awake and freely-moving mice (Article 3)
- Aim III: improve quantum yield and imaging brightness of erbium-based rare-earth nanocrystals for high-contrast, whole-body angiography in mice at wavelengths above 1450 nm (Article 4)
- Aimg IV: enhance the photophysical performance of thulium-based rare-earth nanocrystals for high-contrast, deep imaging at wavelengths between 1600 and 2000 nm (Article 5).
- Aim V: develop and evaluate the potential of SWIR-emitting fluorescent proteins for non-invasive deep-tissue imaging (Article 6)
- Aim VI: study the autofluorescence profile of biological tissue at excitation wavelengths between 785 and 1064 nm (Article 7)
- Aim VII: design a SWIR-based Raman imaging system for macroscopic label-free biomedical imaging applications (Article 7)

3 Summary

Biomedical imaging in the shortwave infrared (SWIR) spectral region offers several advantages over visible and near-infrared (NIR) imaging, including reduced tissue scattering, stronger water absorptivity, and lower tissue autofluorescence. These photophysical properties of SWIR imaging allow for deeper tissue penetration, enhanced image contrast, and improved sensitivity of labeled structures. The articles featured in this thesis introduce significant advancements in SWIR imaging technology, with major progress in both contrast agent development and imaging system implementation, which led to novel biological applications.

Articles 1 and 2 introduce SWIR penta- and heptamethine dyes containing flavylium and chromenylium heterocycles with excitation ranges between 785 and 1064 nm and strong SWIR emission. Moreover, these articles explore imaging strategies for fast, multiplexed SWIR imaging, such as the excitation multiplexing approach, which relies on matching the fluorophore absorbance to different NIR or SWIR laser lines, while using a single detection window in the SWIR. Excitation multiplexing allowed for simple and faster imaging systems, while avoiding the drastic differences in tissue contrast observed by different SWIR imaging bands, which are especially related to water absorptivity. This approach, when combined with strategic fluorophore concentration and laser power optimization, enables real-time, multi-color *in vivo* imaging with minimal crosstalk among the dyes. These unprecedented multiplexing capabilities and faster imaging speeds are particularly impactful in **Article 3**, which utilizes the dyes developed in Articles 1 and 2 to demonstrate simultaneous imaging of four different biological structures in freely moving mice.

Articles 4 and 5 highlight major progress in the development of organic dyes, namely erbium- and thulium-based rare-earth nanocrystals. Article 4 highlights that, by employing a heterogeneous shell domain, a quantum yield of 50% for sub-15 nm erbium-based nanocrystals can be reached. This increase in brightness enables high-contrast vascular imaging in *vivo* with fluorescence emission above 1450 nm, which benefits from high water absorptivity to enhance image contrast by absorbing background fluorescence and scattered light. This study exploits differences in vascular kinetics following intravenous injection to achieve multi-color angiography images of the mouse's whole body, providing a comprehensive visualization of vascular structures with striking imaging definition. Moreover, Article 5 introduces thulium-doped nanocrystals optimized for imaging in the extended SWIR range of 1600 to 2000 nm, achieving an unprecedented 39% quantum yield. This article demonstrates the advantages of imaging depth and contrast associated with fluorescence in this spectral region, with studies in tissue phantoms indicating penetration up to 1 cm. These results and the imaging system designed for extended SWIR imaging establish a foundation for exploring deeper biological imaging applications in an underutilized SWIR spectral window.

Article 6 introduces pioneering developments in the field of SWIR-emitting fluorescent proteins, an underexplored research field. This study presents a novel protein engineered to bind a synthetic merocyanine dye, which can be excited at 892 nm. Moreover, this SWIR protein demonstrates higher contrast and *in vivo* imaging sensitivity compared to the previously established NIR

fluorescent protein, iRFP720, which has an excitation peak around 700 nm. These findings highlight the substantial benefits of employing longer excitation wavelengths, offering enhanced imaging performance and opening new possibilities for deep-tissue non-invasive *in vivo* imaging using genetically encoded fluorescent proteins.

Article 7 introduces the groundbreaking discovery that, at illumination wavelengths equal to or above 892 nm, SWIR autofluorescence is so low that spontaneous Raman scattering, a very weak scattering process, surpasses it as the major source of tissue background. In this article, a wide-field SWIR Raman system is designed, enabling label-free applications such as *in vivo* tracking of body composition dynamics and non-invasive detection of fatty liver disease in mice, visualization of calcification and lipids in fresh human atherosclerotic plaques, as well as identification of nerves embedded in fatty tissue of a porcine surgery model. SWIR Raman imaging enables excellent chemical contrast at an unprecedented spatial scale, overcoming a major limitation in other Raman imaging methods, and opening up new avenues in biomedical imaging.

Overall, the research presented in this thesis provides a significant contribution to the SWIR biomedical imaging field, not only enhancing imaging performance and multiplexing capabilities but also expanding the potential for non-invasive, high-contrast imaging in various biological applications. The advancements in contrast agents, fluorescent proteins, and macroscopic Raman imaging technologies highlight the diverse possibilities SWIR imaging offers for deep tissue visualization and the study of complex biological processes. Altogether, this work paves the way for further innovations in SWIR imaging in both clinical and pre-clinical settings.

4 Zusammenfassung

Die biomedizinische Bildgebung im kurzwelligen Infrarot (SWIR) bietet mehrere Vorteile gegenüber der Bildgebung im sichtbaren und nahen Infrarot (NIR), darunter eine geringere Gewebestreuung, ein stärkeres Wasserabsorptionsvermögen und eine geringere Autofluoreszenz des Gewebes. Diese photophysikalischen Eigenschaften der SWIR-Bildgebung ermöglichen eine tiefere Gewebedurchdringung, einen besseren Bildkontrast und eine höhere Empfindlichkeit der markierten Strukturen. Die Artikel in dieser Arbeit stellen bedeutende Fortschritte in der SWIR-Bildgebungstechnologie vor, mit großen Fortschritten sowohl bei der Entwicklung von Kontrastmitteln als auch bei der Implementierung von Bildgebungssystemen, die zu neuen biologischen Anwendungen führten.

In den **Artikeln 1 und 2** werden SWIR-Penta- und Heptamethin-Farbstoffe vorgestellt, die Flavylium- und Chromenylium-Heterozyklen mit Anregungsbereichen zwischen 785 und 1064 nm und starker SWIR-Emission enthalten. Darüber hinaus werden in diesen Artikeln Bildgebungsstrategien für eine schnelle, gemultiplexte SWIR-Bildgebung untersucht, wie z. B. das Anregungsmultiplexing, bei dem die Absorption des Fluorophors auf verschiedene NIR- oder SWIR-Laserlinien abgestimmt wird, während ein einziges Detektionsfenster im SWIR verwendet wird. Das Anregungsmultiplexing ermöglicht einfache und schnellere Bildgebungssysteme und vermeidet gleichzeitig die drastischen Unterschiede im Gewebekontrast, die bei verschiedenen SWIR-Bildgebungsbändern beobachtet werden und insbesondere mit der Wasserabsorptionsfähigkeit zusammenhängen. In Kombination mit einer strategischen Fluorophor-Konzentration und der Optimierung der Laserleistung ermöglicht dieser Ansatz eine mehrfarbige In-vivo-Bildgebung in Echtzeit mit minimalem Übersprechen zwischen den Farbstoffen. Diese beispiellosen Multiplexing-Fähigkeiten und schnelleren Bildgebungsgeschwindigkeiten kommen besonders in **Artikel 3** zum Tragen, in dem die in den Artikeln 1 und 2 entwickelten Farbstoffe verwendet werden, um die gleichzeitige Bildgebung von vier verschiedenen biologischen Strukturen in frei beweglichen Mäusen zu demonstrieren.

In den **Artikeln 4 und 5** werden wichtige Fortschritte bei der Entwicklung organischer Farbstoffe, insbesondere Nanokristalle auf Erbium- und Thuliumbasis, hervorgehoben. In Artikel 4 wird aufgezeigt, dass durch den Einsatz einer heterogenen Schalendomäne eine Quantenausbeute von 50 % für Nanokristalle auf Erbiumbasis mit einer Größe von unter 15 nm erreicht werden kann. Diese Helligkeitssteigerung ermöglicht eine kontrastreiche Gefäßdarstellung in vivo mit einer Fluoreszenzemission über 1450 nm, die von der hohen Wasserabsorptionsfähigkeit profitiert, um den Bildkontrast durch Absorption von Hintergrundfluoreszenz und Streulicht zu verbessern. In dieser Studie werden die Unterschiede in der Gefäßkinetik nach intravenöser Injektion genutzt, um mehrfarbige Angiographiebilder des gesamten Mauskörpers zu erhalten, die eine umfassende Visualisierung der Gefäßstrukturen mit beeindruckender Bildschärfe ermöglichen. Darüber hinaus werden in Artikel 5 Thulium-dotierte Nanokristalle vorgestellt, die für die Bildgebung im erweiterten SWIR-Bereich von 1600 bis 2000 nm optimiert sind und eine noch nie dagewesene Quantenausbeute von 39 % erzielen. Dieser Artikel demonstriert die Vorteile der Bildgebungstiefe und des Kontrasts, die mit der Fluoreszenz in diesem Spektralbereich verbunden sind, mit Studien in Gewebephantomen, die eine Eindringtiefe von bis zu 1 cm zeigen. Diese Ergebnisse und das

für die erweiterte SWIR-Bildgebung konzipierte Bildgebungssystem bilden eine Grundlage für die Erforschung tieferer biologischer Bildgebungsanwendungen in einem wenig genutzten SWIR-Spektralfenster.

In **Artikel 6** werden bahnbrechende Entwicklungen auf dem Gebiet der SWIR-emittierenden fluoreszierenden Proteine vorgestellt, einem bisher wenig erforschten Forschungsgebiet. In dieser Studie wird ein neuartiges Protein vorgestellt, das so entwickelt wurde, dass es einen synthetischen Merocyanin-Farbstoff bindet, der bei 892 nm angeregt werden kann. Darüber hinaus zeigt dieses SWIR-Protein einen höheren Kontrast und eine höhere Empfindlichkeit bei der In-vivo-Bildgebung im Vergleich zu dem bereits etablierten NIR-Fluoreszenzprotein iRFP720, das einen Anregungspeak bei 700 nm aufweist. Diese Ergebnisse unterstreichen die erheblichen Vorteile der Verwendung längerer Anregungswellenlängen, die eine verbesserte Bildgebungsleistung bieten und neue Möglichkeiten für die nicht-invasive In-vivo-Bildgebung in der Tiefe des Gewebes unter Verwendung genetisch kodierter fluoreszierender Proteine eröffnen.

In **Artikel 7** wird die bedeutende Entdeckung vorgestellt, dass bei Beleuchtungswellenlängen von 892 nm oder mehr die SWIR-Autofluoreszenz so gering ist, dass die spontane Raman-Streuung, ein sehr schwacher Streuprozess, sie als Hauptquelle des Gewebeuntergrunds übertrifft. In diesem Artikel wird ein Weitwinkel-SWIR-Raman-System entwickelt, das markierungsfreie Anwendungen ermöglicht, wie z. B. die In-vivo-Verfolgung der Dynamik der Körperzusammensetzung, die nicht-invasive Erkennung von Fettlebererkrankungen bei Mäusen, die Visualisierung von Verkalkung und Lipiden in frischen menschlichen atherosklerotischen Plaques sowie die Identifizierung von in Fettgewebe eingebetteten Nerven in einem chirurgischen Schweinemodell. Die SWIR-Raman-Bildgebung ermöglicht einen ausgezeichneten chemischen Kontrast in einem noch nie dagewesenen räumlichen Maßstab, wodurch eine wesentliche Einschränkung anderer Raman-Bildgebungsmethoden überwunden und neue Wege in der biomedizinischen Bildgebung beschritten werden.

Insgesamt leisten die in dieser Arbeit vorgestellten Forschungsarbeiten einen bedeutenden Beitrag zur biomedizinischen SWIR-Bildgebung, indem sie nicht nur die Bildgebungsleistung und die Multiplexing-Möglichkeiten verbessern, sondern auch das Potenzial für nicht-invasive, kontrastreiche Bildgebung in verschiedenen biologischen Anwendungen erweitern. Die Fortschritte bei Kontrastmitteln, fluoreszierenden Proteinen und makroskopischen Raman-Imaging-Technologien unterstreichen die vielfältigen Möglichkeiten, die die SWIR-Bildgebung für die Visualisierung von tiefem Gewebe und die Untersuchung komplexer biologischer Prozesse bietet. Insgesamt ebnet diese Arbeit den Weg für weitere Innovationen in der SWIR-Bildgebung sowohl im klinischen als auch im präklinischen Bereich.

First draft translated with DeepL (https://www.deepl.com/en/translator)

5 Article 1

Shortwave infrared polymethine fluorophores matched to excitation lasers enable non-invasive, multicolour *in vivo* imaging in real time

Cosco ED, Spearman AL, Ramakrishnan S, Lingg JGP, Saccomano M, Pengshung M, Arús BA, Wong KCY, Glasl S, Ntziachristos V, Warmer M, McLaughlin RR, Bruns OT, Sletten EM

Nature Chemistry. 2020, *12*(12), 1123-1130.

DOI: https://doi.org/10.1038/s41557-020-00554-5

6 Article 2

Bright chromenylium polymethine dyes enable fast, four-color *in vivo* imaging with shortwave infrared detection

Cosco ED, Arús BA, Spearman AL, Atallah TL, Lim I, Leland OS, Caram JR, Bischof TS, Bruns OT, Sletten EM

Journal of the American Chemical Society. 2021, *143*(18), 6836-6846.

DOI: https://doi.org/10.1021/jacs.0c11599

7 Article 3

Shortwave infrared fluorescence imaging of peripheral organs in awake and freely moving mice

Arús BA, Cosco ED, Yiu J, Balba I, Bischof TS, Sletten EM, Bruns OT.

Frontiers in Neuroscience. 2023, 17, 1135494.

DOI: https://doi.org/10.3389/fnins.2023.1135494

8 Article 4

Preventing cation intermixing enables 50% quantum yield in sub-15 nm short-wave infrared-emitting rare-earth based core-shell nanocrystals

Arteaga Cardona F, Jain N, Popescu R, Busko D, Madirov E, Arús BA, Gerthsen D, De Backer A, Bals S, Bruns OT, Chmyrov A, Van Aert S, Richards BS, Hudry D

Nature Communications. 2023, *14*(1), 4462.

DOI: https://doi.org/10.1038/s41467-023-40031-4

9 Article 5

Dramatic impact of materials combinations on the chemical organization of core–shell nanocrystals: boosting the Tm^{3+} emission above 1600 nm

Arteaga Cardona F, Madirov E, Popescu R, Wang D, Busko D, Ectors D, Kübel C, Eggeler YM, Arús BA, Chmyrov A, Bruns OT, Richards BS, Hudry D

ACS Nano. 2024, 18(38), 26233–26250.

DOI: https://doi.org/10.1021/acsnano.4c07932

References

Alander, J. T., I. Kaartinen, A. Laakso, T. Patila, T. Spillmann, V. V. Tuchin, M. Venermo and P. Valisuo (2012). "A review of indocyanine green fluorescent imaging in surgery." Int J Biomed Imaging **2012**: 940585.

Bandi, V. G., M. P. Luciano, M. Saccomano, N. L. Patel, T. S. Bischof, J. G. P. Lingg, P. T. Tsrunchev, M. N. Nix, B. Ruehle, C. Sanders, L. Riffle, C. M. Robinson, S. Difilippantonio, J. D. Kalen, U. Resch-Genger, J. Ivanic, O. T. Bruns and M. J. Schnermann (2022). "Targeted multicolor in vivo imaging over 1,000 nm enabled by nonamethine cyanines." Nat Methods **19**(3): 353-358.

Blua, F., M. Boccalon, B. Rolando, R. Napolitano, F. Arena, F. Blasi and M. Bertinaria (2024). "Exploring flavylium-based SWIR emitters: Design, synthesis and optical characterization of dyes derivatized with polar moieties." Bioorg Chem **148**: 107462.

Bohndiek, S. E., A. Wagadarikar, C. L. Zavaleta, D. Van de Sompel, E. Garai, J. V. Jokerst, S. Yazdanfar and S. S. Gambhir (2013). "A small animal Raman instrument for rapid, wide-area, spectroscopic imaging." Proc Natl Acad Sci U S A **110**(30): 12408-12413.

Carr, J. A., M. Aellen, D. Franke, P. T. C. So, O. T. Bruns and M. G. Bawendi (2018). "Absorption by water increases fluorescence image contrast of biological tissue in the shortwave infrared." Proc Natl Acad Sci U S A **115**(37): 9080-9085.

Carr, J. A., D. Franke, J. R. Caram, C. F. Perkinson, M. Saif, V. Askoxylakis, M. Datta, D. Fukumura, R. K. Jain, M. G. Bawendi and O. T. Bruns (2018). "Shortwave infrared fluorescence imaging with the clinically approved near-infrared dye indocyanine green." Proc Natl Acad Sci U S A **115**(17): 4465-4470.

Chen, M., Z. Feng, X. Fan, J. Sun, W. Geng, T. Wu, J. Sheng, J. Qian and Z. Xu (2022). "Long-term monitoring of intravital biological processes using fluorescent protein-assisted NIR-II imaging." Nat Commun **13**(1): 6643.

Chen, Y., S. Wang and F. Zhang (2023). "Near-infrared luminescence high-contrast in vivo biomedical imaging." Nature Reviews Bioengineering **1**(1): 60-78.

Cheng, H., H. Xu, B. Peng, X. Huang, Y. Hu, C. Zheng and Z. Zhang (2024). "Illuminating the future of precision cancer surgery with fluorescence imaging and artificial intelligence convergence." NPJ Precis Oncol **8**(1): 196.

Chudakov, D. M., M. V. Matz, S. Lukyanov and K. A. Lukyanov (2010). "Fluorescent proteins and their applications in imaging living cells and tissues." Physiol Rev **90**(3): 1103-1163.

Cialla-May, D., M. Schmitt and J. Popp (2019). "Theoretical principles of Raman spectroscopy." Physical Sciences Reviews **4**(6).

Cosco, E. D., J. R. Caram, O. T. Bruns, D. Franke, R. A. Day, E. P. Farr, M. G. Bawendi and E. M. Sletten (2017). "Flavylium Polymethine Fluorophores for Near- and Shortwave Infrared Imaging." Angew Chem Int Ed Engl **56**(42): 13126-13129.

Croce, A. C. and G. Bottiroli (2014). "Autofluorescence spectroscopy and imaging: a tool for biomedical research and diagnosis." Eur J Histochem **58**(4): 2461.

del Rosal, B. and A. Benayas (2018). "Strategies to Overcome Autofluorescence in Nanoprobe-Driven In Vivo Fluorescence Imaging." Small Methods **2**(9): 1800075.

del Rosal, B., G. Thomas, A. Mahadevan-Jansen and P. R. Stoddart (2020). NIR Autofluorescence: Molecular Origins and Emerging Clinical Applications. Near Infrared-Emitting Nanoparticles for Biomedical Applications. A. Benayas, E. Hemmer, G. Hong and D. Jaque. Cham, Springer International Publishing**:** 21-47.

Del Rosal, B., I. Villa, D. Jaque and F. Sanz-Rodriguez (2016). "In vivo autofluorescence in the biological windows: the role of pigmentation." J Biophotonics **9**(10): 1059-1067.
Ding, F., Y. Zhan, X. Lu and Y. Sun (2018). "Recent advances in near-infrared II fluorophores for multifunctional biomedical imaging." Chem Sci **9**(19): 4370-4380.
Filonov, G. S., K. D. Piatkevich, L. M. Ting, J. Zhang, K. Kim and V. V. Verkhusha (2011). "Bright and stable near-infrared fluorescent protein for in vivo imaging." Nat Biotechnol **29**(8): 757-761.
Frangioni, J. V. (2003). "In vivo near-infrared fluorescence imaging." Curr Opin Chem Biol **7**(5): 626-634.
Freudiger, C. W., W. Min, B. G. Saar, S. Lu, G. R. Holtom, C. He, J. C. Tsai, J. X. Kang and X. S. Xie (2008). "Label-free biomedical imaging with high sensitivity by stimulated Raman scattering microscopy." Science **322**(5909): 1857-1861.
Grimm, J. B. and L. D. Lavis (2022). "Caveat fluorophore: an insiders' guide to small-molecule fluorescent labels." Nat Methods **19**(2): 149-158.
Heuvelings, D. J. I., M. Scheepers, Z. Al-Difaie, N. Okamoto, M. Diana, L. P. S. Stassen, N. D. Bouvy and M. Al-Taher (2024). "Quantitative analysis of intestinal perfusion with indocyanine green (ICG) and methylene blue (MB) using a single clinically approved fluorescence imaging system: a demonstration in a porcine model." Surg Endosc **38**(7): 3556-3563.
Hoffman, R. M. (2005). "The multiple uses of fluorescent proteins to visualize cancer in vivo." Nat Rev Cancer **5**(10): 796-806.
Hong, G., S. Diao, J. Chang, A. L. Antaris, C. Chen, B. Zhang, S. Zhao, D. N. Atochin, P. L. Huang, K. I. Andreasson, C. J. Kuo and H. Dai (2014). "Through-skull fluorescence imaging of the brain in a new near-infrared window." Nat Photonics **8**(9): 723-730.
Hu, F., L. Shi and W. Min (2019). "Biological imaging of chemical bonds by stimulated Raman scattering microscopy." Nat Methods **16**(9): 830-842.
Hu, Z., C. Fang, B. Li, Z. Zhang, C. Cao, M. Cai, S. Su, X. Sun, X. Shi, C. Li, T. Zhou, Y. Zhang, C. Chi, P. He, X. Xia, Y. Chen, S. S. Gambhir, Z. Cheng and J. Tian (2020). "First-in-human liver-tumour surgery guided by multispectral fluorescence imaging in the visible and near-infrared-I/II windows." Nat Biomed Eng **4**(3): 259-271.
James, M. L. and S. S. Gambhir (2012). "A molecular imaging primer: modalities, imaging agents, and applications." Physiol Rev **92**(2): 897-965.
Jermyn, M., K. Mok, J. Mercier, J. Desroches, J. Pichette, K. Saint-Arnaud, L. Bernstein, M. C. Guiot, K. Petrecca and F. Leblond (2015). "Intraoperative brain cancer detection with Raman spectroscopy in humans." Sci Transl Med **7**(274): 274ra219.
Judy, R. P., J. J. Keating, E. M. DeJesus, J. X. Jiang, O. T. Okusanya, S. Nie, D. E. Holt, S. P. Arlauckas, P. S. Low, E. J. Delikatny and S. Singhal (2015). "Quantification of tumor fluorescence during intraoperative optical cancer imaging." Sci Rep **5**: 16208.
Kong, K., C. Kendall, N. Stone and I. Notingher (2015). "Raman spectroscopy for medical diagnostics--From in-vitro biofluid assays to in-vivo cancer detection." Adv Drug Deliv Rev **89**: 121-134.
Krafft, C., I. W. Schie, T. Meyer, M. Schmitt and J. Popp (2016). "Developments in spontaneous and coherent Raman scattering microscopic imaging for biomedical applications." Chem Soc Rev **45**(7): 1819-1849.
Lakowicz, J. R. (2006). Principles of fluorescence spectroscopy. New York, Springer.
Liu, Y., Y. Li, S. Koo, Y. Sun, Y. Liu, X. Liu, Y. Pan, Z. Zhang, M. Du, S. Lu, X. Qiao, J. Gao, X. Wang, Z. Deng, X. Meng, Y. Xiao, J. S. Kim and X. Hong (2022). "Versatile Types of

Inorganic/Organic NIR-IIa/IIb Fluorophores: From Strategic Design toward Molecular Imaging and Theranostics." Chem Rev **122**(1): 209-268.
Martin, A. and P. Rivera-Fuentes (2024). "A general strategy to develop fluorogenic polymethine dyes for bioimaging." Nat Chem **16**(1): 28-35.
Mieog, J. S. D., F. B. Achterberg, A. Zlitni, M. Hutteman, J. Burggraaf, R. J. Swijnenburg, S. Gioux and A. L. Vahrmeijer (2022). "Fundamentals and developments in fluorescence-guided cancer surgery." Nat Rev Clin Oncol **19**(1): 9-22.
Okamoto, N., Z. Al-Difaie, M. Scheepers, D. J. I. Heuvelings, M. R. Rodriguez-Luna, J. Marescaux, M. Diana, L. P. S. Stassen, N. D. Bouvy and M. Al-Taher (2023). "Simultaneous, Multi-Channel, Near-Infrared Fluorescence Visualization of Mesenteric Lymph Nodes Using Indocyanine Green and Methylene Blue: A Demonstration in a Porcine Model." Diagnostics (Basel) **13**(8).
Oliinyk, O. S., C. Ma, S. Pletnev, M. Baloban, C. Taboada, H. Sheng, J. Yao and V. V. Verkhusha (2023). "Deep-tissue SWIR imaging using rationally designed small red-shifted near-infrared fluorescent protein." Nat Methods **20**(1): 70-74.
Orringer, D. A., B. Pandian, Y. S. Niknafs, T. C. Hollon, J. Boyle, S. Lewis, M. Garrard, S. L. Hervey-Jumper, H. J. L. Garton, C. O. Maher, J. A. Heth, O. Sagher, D. A. Wilkinson, M. Snuderl, S. Venneti, S. H. Ramkissoon, K. A. McFadden, A. Fisher-Hubbard, A. P. Lieberman, T. D. Johnson, X. S. Xie, J. K. Trautman, C. W. Freudiger and S. Camelo-Piragua (2017). "Rapid intraoperative histology of unprocessed surgical specimens via fibre-laser-based stimulated Raman scattering microscopy." Nat Biomed Eng **1**.
Ou, Y.-F., T.-B. Ren, L. Yuan and X.-B. Zhang (2023). "Molecular Design of NIR-II Polymethine Fluorophores for Bioimaging and Biosensing." Chemical & Biomedical Imaging **1**(3): 220-233.
Palonpon, A. F., J. Ando, H. Yamakoshi, K. Dodo, M. Sodeoka, S. Kawata and K. Fujita (2013). "Raman and SERS microscopy for molecular imaging of live cells." Nat Protoc **8**(4): 677-692.
Papour, A., J. H. Kwak, Z. Taylor, B. Wu, O. Stafsudd and W. Grundfest (2015). "Wide-field Raman imaging for bone detection in tissue." Biomed Opt Express **6**(10): 3892-3897.
Patil, C. A., I. J. Pence, C. A. Lieber and A. Mahadevan-Jansen (2014). "1064 nm dispersive Raman spectroscopy of tissues with strong near-infrared autofluorescence." Opt Lett **39**(2): 303-306.
Piwonski, H., S. Nozue and S. Habuchi (2022). "The Pursuit of Shortwave Infrared-Emitting Nanoparticles with Bright Fluorescence through Molecular Design and Excited-State Engineering of Molecular Aggregates." ACS Nanosci Au **2**(4): 253-283.
Refaat, A., M. L. Yap, G. Pietersz, A. P. G. Walsh, J. Zeller, B. Del Rosal, X. Wang and K. Peter (2022). "In vivo fluorescence imaging: success in preclinical imaging paves the way for clinical applications." J Nanobiotechnology **20**(1): 450.
Resch-Genger, U., M. Grabolle, S. Cavaliere-Jaricot, R. Nitschke and T. Nann (2008). "Quantum dots versus organic dyes as fluorescent labels." Nat Methods **5**(9): 763-775.
Rodriguez, E. A., R. E. Campbell, J. Y. Lin, M. Z. Lin, A. Miyawaki, A. E. Palmer, X. Shu, J. Zhang and R. Y. Tsien (2017). "The Growing and Glowing Toolbox of Fluorescent and Photoactive Proteins." Trends Biochem Sci **42**(2): 111-129.
Schmidt, E. L., Z. Ou, E. Ximendes, H. Cui, C. H. C. Keck, D. Jaque and G. Hong (2024). "Near-infrared II fluorescence imaging." Nature Reviews Methods Primers **4**(1): 23.
Sun, Y., X. Zhong and A. M. Dennis (2023). "Minimizing near-infrared autofluorescence in preclinical imaging with diet and wavelength selection." J Biomed Opt **28**(9): 094805.

Uranga-Barandiaran, O., D. Casanova and F. Castet (2020). "Flavylium Fluorophores as Near-Infrared Emitters." Chemphyschem **21**(20): 2243-2248.
Wallyn, J., N. Anton, S. Akram and T. F. Vandamme (2019). "Biomedical Imaging: Principles, Technologies, Clinical Aspects, Contrast Agents, Limitations and Future Trends in Nanomedicines." Pharm Res **36**(6): 78.
Wang, F., Y. Zhong, O. Bruns, Y. Liang and H. Dai (2024). "In vivo NIR-II fluorescence imaging for biology and medicine." Nature Photonics.
Webb, A. (2022). Introduction to biomedical imaging, John Wiley & Sons.
Wei, D., S. Chen, Y. H. Ong, C. Perlaki and Q. Liu (2016). "Fast wide-field Raman spectroscopic imaging based on simultaneous multi-channel image acquisition and Wiener estimation." Opt Lett **41**(12): 2783-2786.
Weissleder, R. and M. Nahrendorf (2015). "Advancing biomedical imaging." Proc Natl Acad Sci U S A **112**(47): 14424-14428.
Welsher, K., Z. Liu, S. P. Sherlock, J. T. Robinson, Z. Chen, D. Daranciang and H. Dai (2009). "A route to brightly fluorescent carbon nanotubes for near-infrared imaging in mice." Nat Nanotechnol **4**(11): 773-780.
Wilson, B. C., M. Jermyn and F. Leblond (2018). "Challenges and opportunities in clinical translation of biomedical optical spectroscopy and imaging." J Biomed Opt **23**(3): 1-13.
Wilson, R. H., K. P. Nadeau, F. B. Jaworski, B. J. Tromberg and A. J. Durkin (2015). "Review of short-wave infrared spectroscopy and imaging methods for biological tissue characterization." J Biomed Opt **20**(3): 030901.
Wu, Y., Y. Suo, Z. Wang, Y. Yu, S. Duan, H. Liu, B. Qi, C. Jian, X. Hu, D. Zhang, A. Yu and Z. Cheng (2022). "First clinical applications for the NIR-II imaging with ICG in microsurgery." Front Bioeng Biotechnol **10**: 1042546.
Yang, S., B. Li, A. Akkus, O. Akkus and L. Lang (2014). "Wide-field Raman imaging of dental lesions." Analyst **139**(12): 3107-3114.
Zhang, R. R., A. B. Schroeder, J. J. Grudzinski, E. L. Rosenthal, J. M. Warram, A. N. Pinchuk, K. W. Eliceiri, J. S. Kuo and J. P. Weichert (2017). "Beyond the margins: real-time detection of cancer using targeted fluorophores." Nat Rev Clin Oncol **14**(6): 347-364.
Zhong, X., A. Patel, Y. Sun, A. M. Saeboe and A. M. Dennis (2024). "Multiplexed Shortwave Infrared Imaging Highlights Anatomical Structures in Mice." Angew Chem Int Ed Engl **63**(43): e202410936.
Zhu, B., S. Kwon, J. C. Rasmussen, M. Litorja and E. M. Sevick-Muraca (2020). "Comparison of NIR Versus SWIR Fluorescence Image Device Performance Using Working Standards Calibrated With SI Units." IEEE Trans Med Imaging **39**(4): 944-951.
Zhu, S., R. Tian, A. L. Antaris, X. Chen and H. Dai (2019). "Near-Infrared-II Molecular Dyes for Cancer Imaging and Surgery." Adv Mater: e1900321.

Appendix A: Article 6

De novo design of near infrared fluorescent proteins

Xu C*, Liu Y*, Arús BA*, Mishra K*, Luciano M, Bandi V, Kumar A, Guo Z, Bick M, Xu M, Zhang K, Lingg J, Bae J, Kang A, Gerben SR, Bera AK, Vaughan JC, Manton JD, Derivery E, Schnermann MJ, Stiel AC, Bruns OT, Baker D

Research Square. 2024, 4652998.

DOI: https://doi.org/10.21203/rs.3.rs-4652998/v1

* shared first authorship

Appendix B: Article 7

Macroscopic label-free biomedical imaging with shortwave infrared Raman scattering

Arús BA, Yiu J, Lingg JGP, Hofmann A, Fumo AR, Ji H, Jethwa C, Park R K, Henderson J, Mishra K, Mukha I, Stiel AC, Santovito D, Weber C, Reeps C, Rohm M, Bartelt A, Valdez TA, Chmyrov A, Bruns OT

bioRxiv. 2024, 10597863.

DOI: https://doi.org/10.1101/2024.06.10.597863

Acknowledgments

Throughout the journey developing this thesis, my academic and personal growth has been shaped by remarkable people who have guided, supported, and inspired me over the years. I am incredibly thankful to my mentors, colleagues, and collaborators, as well as for the privilege of conducting my doctorate at leading institutions that provided me with outstanding infrastructure and support.

First, I would like to express my sincere gratitude to Oliver Bruns for his belief in my potential and for welcoming me into his lab. His constant support, guidance, and encouragement to explore a variety of projects and technologies have been absolutely essential to my development. I admire Oliver's big-picture vision and his honest, open communication, which set a great example of excellence-driven leadership with kindness.

I am also very thankful to Alexander Bartelt for taking me on as his PhD student and for the opportunities we have had to collaborate. Alex's ambitious drive and strategic thinking have been extremely formative and inspiring for me.

Additionally, I am genuinely grateful for the mentorship of Andriy Chmyrov and Thomas Bischof. Both have challenged me to broaden my skills and knowledge into areas I had not foreseen before joining the lab. Their patient teachings, huge support, and deep discussions have left a very significant impact on my academic path.

To all the former and current members of the Bruns lab, thank you for your camaraderie, collaboration, and support throughout this journey. I am especially grateful to have had Maly Cosco and Joycelyn Yiu as lab mates. Maly's contagious motivation made working together absolutely fun, while her knowledge and skills were fundamental in helping me learn and adapt quickly during my early years in the lab. Joycelyn's dedication, tireless energy, and eagerness to learn were equally inspiring and a joy to share (no pun intended). With both of them, I had some of the most memorable and rewarding experiences – and experiments – of my academic life.

Further sincere thanks go to Martin Warmer for his exceptional expertise, guidance and assistance, as well as to Jakob Lingg, Mara Saccomano, Merle Weitzenberg, Iuliia Mukha and Simon Härtl for our shared experiences, discussions, and close collaboration. Another very special thank you goes to Maria Voigt for her remarkably dedicated assistance to keep our work running smoothly.

Working in such a multidisciplinary field has been a true satisfaction and source of growth. Accordingly, I am immensely thankful to all my external collaborators, whose insights and contributions were absolutely essential to the success of this research. I would like to particularly thank Ellen Sletten and Tulio Valdez for their mentorship and guidance, as well as Damien Hudry, Chunfu Xu, Maria Rohm, Anja Hofmann, Donato Santovito, Fernando Arteaga Cardona, and Carolin Jetwha for their invaluable contributions to our shared projects.

Finally, to my family, thank you for your huge support throughout my entire journey, regardless of the distance that separates us. And to Luisa, my amazing partner, I am so grateful for the happiness, encouragement, support, and strength that you add to my life every day.